Visualization of Intricate Flow Structures for Vortex Breakdown Analysis

Xavier Tricoche* University of Utah
Christoph Garth University of Kaiserslautern
Gordon Kindlmann University of Utah
Eduard Deines University of Kaiserslautern
Gerik Scheuermann University of Leipzig
Markus Ruetten DLR Goettingen
Charles Hansen University of Utah

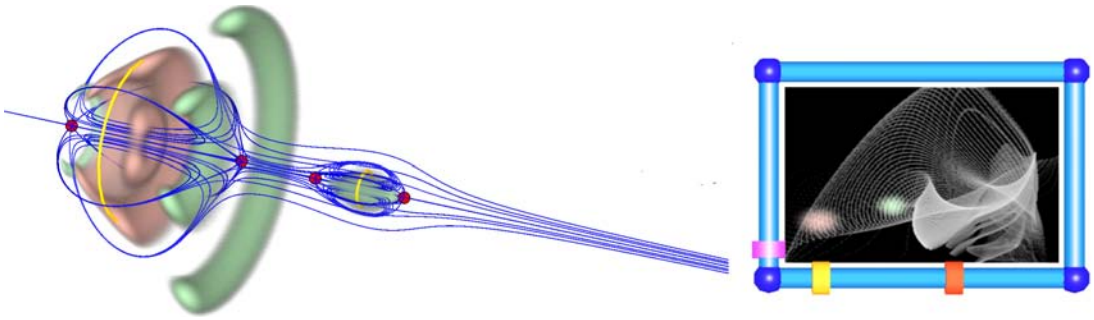

Figure 1: Vortex breakdown bubble in numerical simulation of a cylindrical container. Flow topology is illustrated with stagnation points (red), singularity paths (yellow), and streamlines (blue) on three axially oriented cutting planes. Volume rendering illustrates additional aspects of flow structure, using a two-dimensional transfer function (widget, right) of a Jacobian-related invariant (horizontal axis) and vorticity (vertical axis).

Abstract

Vortex breakdowns and flow recirculation are essential phenomena in aeronautics where they appear as a limiting factor in the design of modern aircrafts. Because of the inherent intricacy of these features, standard flow visualization techniques typically yield cluttered depictions. The paper addresses the challenges raised by the visual exploration and validation of two CFD simulations involving vortex breakdown. To permit accurate and insightful visualization we propose a new approach that unfolds the geometry of the breakdown region by letting a plane travel through the structure along a curve. We track the continuous evolution of the associated projected vector field using the theoretical framework of parametric topology. To improve the understanding of the spatial relationship between the resulting curves and lines we use direct volume rendering and multi-dimensional transfer functions for the display of flow-derived scalar quantities. This enriches the visualization and provides an intuitive context for the extracted topological information. Our results offer clear, synthetic depictions that permit new insight into the structural properties of vortex breakdowns.

CR Categories: I.4.7 [Image Processing and Computer Vision]: Feature Measurement— [I.6.6]: Simulation And Modeling— Simulation Output Analysis J.2 [Physical Sciences and Engineering]: Engineering—.

Keywords: flow visualization, vortex analysis, parametric topology, cutting planes, volume rendering

1 Introduction

Computational Fluid Dynamics (CFD) has become an essential tool in various engineering fields. In aeronautics it is a key element in the design of modern aircrafts. The speed of today's computers combined with the increasing complexity of physical models yields numerical simulations that accurately reproduce the subtle flow structures observed in practical experiments and permit to study their impact on flight stability. Yet, to fully exploit the huge amount of information contained in typical data sets, engineers require post-processing techniques providing insight into the results of their computation.

In order to meet these needs the research in Flow Visualization has designed various methods aimed at efficiently exploring fluid flow data and automatically characterizing their essential properties. Unfortunately, vortex breakdowns and their associated flow recirculation patterns remain challenging structures and none of the existing visualization techniques can offer satisfying depictions of these features. Their truly three-dimensional nature is poorly visualized by conventional methods, such as e.g. streamlines and isosurfaces. Stream surfaces [6] improve on these basic techniques but still obscure the intricate internal structures of recirculation bubbles.

The work described in this paper has its origins in the collaboration between engineering and visualization. The problem posed was to find efficient methods to validate two large simulation datasets and analyze the contained features, with an emphasis on vortices and vortex breakdowns. The approach presented in the following consists in compounding two kinds of visualization techniques that had little interaction so far. More precisely, we associate topology-based flow visualization methods and volume rendering. This provides depictions that both convey the subtle structures present in vortical flows, especially during vortex breakdown, and provide an intuitive understanding of their spatial context and associated physical properties.

The central idea of our flow visualization method is to extend the basic and widely used cutting plane technique to make it a flexible and powerful tool for exploring flow volumes in a continuous way. These *moving cutting planes*, as we term them in this paper, smoothly travel along trajectories that can be either obtained automatically by standard feature extraction schemes or provided by the user to explore a particular region. Building on an existing

*Email: tricoche@sci.utah.edu

IEEE Visualization 2004
October 10-15, Austin, Texas, USA
0-7803-8788-0/04/$20.00 ©2004 IEEE

technique we accurately track the vector field topology observed on the cutting planes. This allows us to detect and visualize essential properties of the flow, especially for recirculation bubbles. Our application of the volume rendering technique is based on the concept of multidimensional transfer functions. In the processing of our data sets this methodology proves extremely useful in permitting the simultaneous and coherent depiction of multiple flow-derived scalar fields, traditionally used to analyze vortical structures. Combined with the topological information gathered by our moving cutting plane this enhances the visualization and facilitates the understanding of both the geometry and the physical properties of our fluid flow data. Observe that although the data at hand are time-dependent we chose to restrict our visualization to the analysis of the structural features contained in individual time steps.

2 Related Work

The study of vortex breakdown is a field of its own in the fluid mechanics community. The corresponding literature mostly uses streamlines or particles advection to observe and analyze the properties of breakdown bubbles [22, 26]. From the viewpoint of Scientific Visualization the phenomenon has not received much attention so far and Kenwright and Haimes [12] published one of the few papers explicitly considering this problem. Vortices, however, are an essential topic of Flow Visualization and have been treated quite extensively. In the absence of a formal characterization of vortical structures, swirling motion around some central region is used as a working definition [20, 24]. Depending on the approach taken, this leads to features that are either lines, surfaces or volumes. Vortex core lines appear to be the most prominent feature type. Banks and Singer [2] extracted them by looking for points with low pressure and high absolute vorticity. Sujudi and Haimes [28] applied a cell-wise linear pattern matching strategy to find vortex core lines over tetrahedral grids. This fast method is probably the most widely used in practice. Peikert and Roth [23] showed that this and most other line-based feature detection methods can be reformulated using the concept of *Parallel Operator*, leading to continuous features. They also proposed a second order method [25]. A famous region-based method is the λ_2-criterion proposed by Jeong and Hussein [9]. It connects a vortical region to the negative eigenvalues of a symmetric matrix derived from the Jacobian. Alternative techniques were introduced recently [10, 6]. Aside from this line of research, vortices are usually characterized by certain physical quantities like pressure, vorticity or helicity. Finding the corresponding regions can then be formulated as a level set problem and reduced to iso-surface extraction. Unfortunately, none of the methods mentioned above is able to deal with the very complex flow behaviors associated with vortex breakdowns.

Although topology-based methods have been widely and successfully applied to the visualization of planar vector fields, the extension of this technique to three-dimensional flows is still incomplete. Early contributions [8, 7] were restricted to the extraction and identification of first-order critical points and the integration of line-type separatrices. Recently, Theisel et al. presented a method for the visualization of so-called saddle connectors [30]. These line-type features avoid occlusion but provide an incomplete structural picture. Mahrous et al. [21] described an approach for the topological segmentation of 3D data sets in which separatrices are obtained as implicit stream surfaces [32]. As a consequence, the accuracy is typically limited in regions of intricate flow. Concerning unsteady data, Tricoche et al. proposed a technique for tracking the topology of planar flows over time [31]. A different approach was introduced later by Theisel and Seidel [29]. The method presented in this paper builds on the original idea of [31].

Direct volume rendering is a powerful tool for the visualization of scalar volumetric data because of its simplicity and flexibility. Its simplicity facilitates interactive implementation on graphics hardware while its flexibility is grounded in its reliance on the transfer function, which maps from data values to the colors and opacities. Additional flexibility comes from transfer functions with a multi-dimensional domain, allowing the rendering to display not just (soft) isosurfaces of individual data values, but the relationships between them. Multi-dimensional transfer functions were pioneered by Levoy [19], generalized by Kindlmann and Durkin [13], and more recently advanced by Kniss et al. for the visualization of scalar datasets [15], as well as for color cryosection data and meteorological simulations [16]. Note that, starting from scalar quantities provided by CFD simulations, Ebert et al. already proposed to use volume rendering for the visualization of gases in [4]. We use a different approach in the following and show how multi-dimensional transfer functions were integrated in our framework to improve the visualization of vortex breakdown structures.

3 CFD Datasets

The following two CFD data sets are the basis of the work presented in this paper. They were both obtained using the DLR Tau Code solver.

Can dataset This simulation corresponds to a cylindrical container of aspect ratio 1 filled with an incompressible and highly viscous liquid. The objective was to study vortex breakdown under ideal conditions (highly viscous fluid and high symmetry in the problem), yielding very accurate and smooth numerical data. The cylinder's top lid rotates, resulting in lid-driven flow showing a vortex on the cylinder symmetry axis. The gradually increased angular velocity of the lid leads to the appearance and successive vanishing of two vortex breakdowns over the 500 time steps. This case has been examined experimentally in great detail [5]. The computational grid contains approximatively 750.000 elements. Available data attributes include velocity, pressure and kinetic energy.

Delta wing This simulation describes a sharp-edged prismatic delta wing at subsonic speed (0.2 mach) with the characteristic vortical systems above the wing. The angle of attack increases over time, eventually leading to vortex breakdown in later timesteps. The viscous simulation of the full configuration was performed without the assumption of symmetry. The grid consists of 11.1 million unstructured grid cells and about 3 million vertices. The variables are the same as previously, provided for 90 time steps. This data set features secondary and tertiary vortices on the wing and corresponding separation and attachment structures.

4 Topological Exploration of Vortical Regions

4.1 Moving Cutting Planes

4.1.1 Trajectories

To visualize both vortices and vortex breakdowns present in our data sets we considered three types of trajectories, each applying to a specific context.

Vortex Core Lines The most natural choice for exploring vortical structures is to follow vortex core lines, i.e. the line-type center of flow rotation. To extract them we use an implementation of the method of Sujudi and Haimes [28] based on the *Parallel Operator* [23]. This method provides satisfying results for the principal vortices in the delta wing dataset. A smoothing step applied in preprocessing was found to improve the results.

Straight Line Alternatively, straight lines across the grid can be selected by the user. This has two major applications. First, if the focus is on large-scale vortices, the mean flow direction in the corresponding region can be selected along with a convenient start

position. We use this technique for visualizing the primary vortices in the delta wing. The second application arises when automatic vortex core extraction fails for a particular vortex but its approximative trajectory is known.

Recirculation Bubble Axis The last type of trajectory directly fits the main feature of our analysis, namely the recirculation bubbles induced by the vortex breakdown. Since this phenomenon entails a dramatic change in the vortex structure, vortex core line extraction cannot be used here. Fortunately, recirculation bubbles, though asymmetric in general, typically exhibit a medium axis corresponding to their overall orientation. More specifically, each recirculation bubble is delimited by two stagnation points and we explore them by rotating the cutting plane around the axis connecting them.

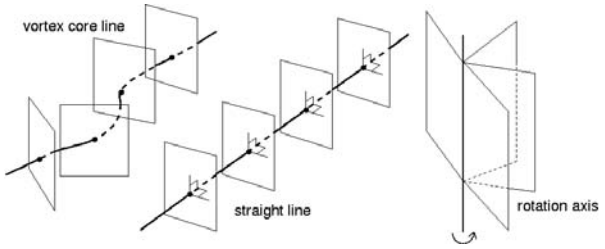

Figure 2: Different types of moving cutting planes

4.1.2 Cutting Plane Orientation

The orientation of the plane is the second critical parameter of our flow exploration technique. It can be seen on Fig. 2 that choosing the recirculation bubble axis as exploratory curve fully determines the plane orientation. Similarly a straight line is also used as plane normal when it is selected to capture large-scale features, as explained previously. In contrast, when dealing with a vortex core line the inaccuracy in the extraction method results in an approximated position of the actual vortex core which can have a negative impact on the resulting normal value. The same holds true when approximating the curved, possibly complex path of a vortex by a straight line segment. In both cases we need an automatic way to compute a suitable normal at each point along the discrete path according to the local flow orientation. Practically, the quality of a normal is evaluated with respect to the amount α of normalized flow crossing the plane, integrated over a small region around the considered point. To maximize this quantity we adopt the following iterative scheme. The plane's normal is initialized as the velocity vector at the considered point along the line. Next the vector field is sampled at a few locations evenly distributed around this point on the initial plane. The mean vector of the normalized sample values is computed along with the corresponding value of α. The mean vector then replaces the current normal in the next iteration. We proceed until no significant improvement of α can be achieved. Observe that more elaborate techniques can be used to determine the plane orientation, like those involving Principal Component Analysis [11, 1], but we found that this simple technique gives very good results.

4.1.3 Planar Resampling

The remaining task consists in resampling the 3D vector field on the cutting plane while ensuring consistency of the coordinate frames between consecutive positions along the followed curve. This is mandatory to obtain meaningful results during the topology tracking procedure described next. To do so, it is sufficient to assign a single basis vector to each plane, the second one being readily obtained by cross product with the normal. Practically we select an arbitrary vector in the first plane and we iteratively transport this vector from one plane to the next by successive projections and renormalization, similar to e.g. [27].

The resulting basis along with a user-prescribed step size allows us to resample the vector field on a raster grid on each cutting plane. The last issue concerns the size of the raster grid. Namely, the radius of the sample grid around the trajectory should be small enough to prevent the inclusion of samples lying outside the considered vortex. Indeed, such samples would lead to topological artifacts and must be avoided. On the other hand, the radius must be large enough to enclose the outer boundary of the vortical region. To solve this problem, our implementation provides two control mechanisms over the radius. The first one consists in letting the user set a constant radius for the whole path. This is convenient if the vortex is well isolated and has a roughly constant shape. A second and more elaborate technique involves a scheme that Garth et al. presented in [6]. In a nutshell, the vortex outer boundary is automatically detected as the curve where the swirl or circumferential velocity is maximum. This allows for non-circular regions with variable radius, which gives us the required flexibility to properly process the data. Given a maximum size for our raster grid we eventually mark every sample point as *invalid* if it lies outside the boundary that we just identified.

4.2 Topology Tracking

The previous step collects the successive values of the projected vector field as the cutting plane moves through the volume. We now abstract them from their original embedding in three-space and consider them as the successive states of a parameter-dependent planar vector field. This construction allows us to apply an existing algorithm for topology tracking of two-dimensional vector fields to the visualization of three-dimensional flow structures. It is equivalent to splitting the continuous three-dimensional physical space of the original data into the two-dimensional space of the cutting plane and the one-dimensional, parametric space of its trajectory.

4.2.1 Planar Vector Field Topology

The topology of a steady, planar vector field (also known as *topological skeleton*) is defined as a graph whose vertices are *critical points* and whose edges are particular streamlines, called *separatrices*. Critical points are positions where the vector field magnitude vanishes. They are classified with respect to the eigenvalues of the Jacobian matrix (the first order derivative of the vector field). Among the existing types only saddle points, spirals and centers are relevant in the scope of the method, see Fig. 3. Separatrices are obtained by integrating the vector field along the eigenvectors of saddle points. Closed streamlines, also called cycles, play a role similar to separatrices.

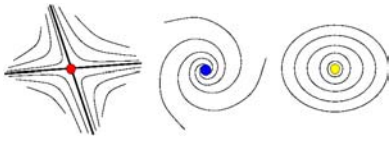

Figure 3: Critical points: saddle, spiral and center point

4.2.2 Tracking Scheme

In the case of a parameter-dependent vector field the structures described previously undergo transformations called bifurcations. To

keep track of the flow structures and monitor their evolution we apply the scheme presented by Tricoche et al. [31]. The basic idea consists in tracking the critical points and associated separatrices over a continuous *space-time* domain spanned by a grid connecting the cells of the planar triangulation over the 1D parameter line. The resulting cells are prisms and a piecewise linear interpolation, both in space and time, of the discrete vector values allows for an efficient computation of the singularities' paths and types on a cell-wise basis. Changes correspond to bifurcations and are easily detected and characterized.

4.2.3 Application to Cutting Plane Topology

We now apply this technique to the vector data gathered along the path of the moving cutting plane. First, we account for the variable size of the sampled region by discarding cells containing a vertex associated with an *invalid* value. Second we have to deal with the lack of smoothness of the vector field projected on the moving cutting plane. This is induced by the technique used to determine the normal of the cutting plane since it does not take into account the normal of the previous planes but rather relies on the local orientation of the flow. Specifically this may cause spiraling critical points to oscillate between sink and source behavior, creating numerous bifurcations. We correct this effect by filtering out low-scale features like pairs of critical points vanishing shortly after their creation or type swap between sources and sinks. The latter is handled by assigning the type *center* to the critical point. Although this is an unstable structure in planar topology, this may be monitored in cutting plane topology when inspecting a vortex whose spiraling flow neither converges nor diverges with respect to its core line.

5 Volume Rendering of Complex Flow Structures

5.1 Sampling

To apply the volume rendering technique to our CFD data sets we first resample them on raster grids - although methods exist that permit volume rendering directly on unstructured grids [18]. This choice is motivated by the extreme complexity of CFD grids and the need for an accurate and robust computation of flow-derived quantities in the next step. However, since the grids at hand exhibit cell sizes varying by up to five orders of magnitude, obtaining a reliable resampling that allows for insightful analysis of the visualization results turns out to be a challenging task.
The technique we applied in this context is based on the idea of scale-space interpolation and organized in three successive steps.

Cell-based Sampling Our flow visualization tool provides a data structure that permits fast data interpolation at any given position inside the grid [17]. This is done by first locating the cell containing the position and then computing a cell-wise interpolation. The grids we considered consist of prisms, pyramids and tetrahedra which implies that the interpolation may be either linear or correspond to some special type of trilinear function. Our cell-based sampling uses this interpolation to collect initial vector values. At the same time we compute the scale of the cell, i.e. its size with respect to the prescribed voxel size. To get a smooth cell scale value over the whole grid we average this cell-centered values around each vertex and apply a cell-wise interpolation of this quantity. Observe that to avoid aliasing artifacts in very small cells we use a jittered sampling technique to average the surrounding values.

Multi-scale Smoothing To prevent artifacts due to visible faces of big cells in the original grid some smoothing is required. This is a critical aspect since derivative computation as described in the next section is going to emphasize such artifacts, leading to very poor results. Yet, the smoothing must be strictly limited to preserve the properties of the original data. Therefore we compute, after sampling, a set of smoothed vector fields with masks of different scales. The range of the mask sizes is chosen to account for all the cell scales encountered during previous sampling. Practically, we use cubic B-spline filters whose support sizes are powers of 2.

Scale Interpolation The last step consists in computing the final sample value as an interpolation of the pre-computed blurred vector fields. To this end we simply use the cell scale values gathered previously to determine the interpolation coefficients in scale space.

5.2 Flow-derived Scalar Quantities

The scalar quantities we compute for volume rendering are those traditionally used in fluid dynamics when investigating vortical phenomena. More precisely we consider divergence, vorticity, helicity (i.e. the dot product of velocity and vorticity), the λ_2 criterion [9], and the imaginary part of the Jacobian eigenvalues. Their common property is to be based on the Jacobian matrix of the vector field which requires derivative computation. To ensure a level of accuracy suited for visualization and analysis, we apply the methodology first presented by Kindlmann et al. [14] that permits the measure of high-quality derivatives by means of convolution filters.

5.3 Multidimensional Transfer Function

We found that multi-dimensional transfer functions are especially effective in visualization of complex flow structures because of the large number of simulation-related variables used to characterize and quantify local properties of the fluid flow data (section 5.2). As observed in previous work [16], having more than two domain variables in the transfer function greatly complicates the user interface, so we have restricted ourselves to two-dimensional transfer functions. Thus, the exploratory visualization process involves (1) finding the pair of CFD variables which proves most effective in capturing important features, and (2) experimenting with transfer functions to highlight different structures, namely vortex system and breakdown bubble.

Non-trivial flow features do not always have simple and universally accepted definitions in terms of numerical properties like vorticity and λ_2. Thus, finding a transfer function which appropriately highlights a region of interest in the flow feature can be a fairly non-intuitive task. We have found that *dual-domain interaction* is a significant benefit. Following previous work [15], we start by placing a cutting plane roughly within the feature of interest. Then, interactive probing (with the cursor) on that plane determines a position in the volume dataset, which in turn determines a point in the transfer function domain. By assigning opacity to a small region around that point, the volume rendering highlights the selected volume position, as well as all other voxels which share its data properties. By moving the cursor into and out of the volume feature, different aspects of its structure are dynamically visualized with the changing transfer function, and the relationship to the pre-computed feature lines can be explored.

6 Results

6.1 Validation

The parametric topology scheme from Section 4.2 was applied to both datasets (cf. 3) with the aim of verifying that the simulations correspond to physical experiments that are similar in nature. Note that we do not claim that our visualization results ensure the correctness or, as in the case of the cylindric container, establish an error in the data. Rather our approach consists in highlighting the existing structures and pointing at problematic aspects of the data

sets that require further investigation, e.g. with other visualization methods.

For the delta wing dataset, the reproduction of primary, secondary and tertiary vortices is crucial. Figure 6 left gives an overview of the wing created with parallel cutting planes along the wing symmetry axis. The primary vortices are presented prominently, and the vortex axis results from the tracking of the corresponding singularities. Using the cutting plane orientation scheme described in Section 4.1.2 with the vortex core as input curve for the plane generation, both secondary and tertiary vortices are visible. Moreover, the planar cut reveals interactions between the three vortices that are hard to determine by other means. This includes the separation surface between the primary and secondary vortices and the so-called *primary separation*, i.e. the flow sheet that emanates from the wing edge and divides the flow above the wing from the surrounding flow. Both appear as a separatrix in the plane.

The dataset had been examined for the presence of the vortical system before, using the method of Sujudi and Haimes [28]. However, this scheme requires careful computation of derivatives and involves smoothing. The result is a set of disconnected line segments and is hard to interpret. In comparison, the approach employed here was easily applied. This can be attributed in part to the fact that the approximate location of the sought features was a priori known, which is usually the case in the verification of datasets.

Application of the planar topology to the can dataset has revealed a peculiarity. The simulation exhibits vortex breakdown, hence a so-called *breakdown bubble* is visible. Over time, this bubble grows, merges and successively re-splits with a second bubble, and shrinks until it vanishes as the breakdown is resolved. The growing of the bubble is attributed to absorption of external material into the bubble (this is sometimes called *feeding*). The reverse process is responsible for the shrinking of the bubble. However, we discovered that for all timesteps in which the bubble is present, a planar cut on the vortex axis reveals that material is leaving the bubble (see Figure 5). This can be seen from the configuration of separatrices. For further illustration, a streamline is started inside the bubble and leaves through the downstream end, both during the growing (left) and shrinking (right) phases. Aside from this, the simulation behaves as expected (see Figure 4). There are two possibilities: either the simulation is wrong (it does not correspond to the sketches of Dallmann[3]), or the feeding is accomplished by a mechanism that cannot be understood from looking at stationary data, which is an interesting statement in itself. The given method has helped in uncovering this anomaly by presenting an intuitive visualization. Although the dataset had been subject to analysis for some time, this had gone unnoticed so far.

Aside from the strict validation of datasets, parametric planar topology can also serve as a feature extraction method for vortex core lines under limited circumstances. For example, the primary vortex axes in the delta wing dataset can be extracted in this manner (cf. Figure 6). Although it is in this case equivalent to other algorithms, it excels in the extraction of recirculation cores. As the vortex breakdown bubble encloses a mostly rotation symmetric region of recirculation, there is essentially a bent vortex inside the bubble. Its core appears as a singularity in the section planes revolving around the original vortex axis. Hence, tracking provides a connection between different planes and thus constructs the core of the recirculation vortex. Figures 4 and 8 show these recirculation rings.

6.2 Volume rendering/grid resampling and in-context visualization

As described in Section 5, subsections of interest (mainly the vortex breakdown regions) of both datasets were resampled and displayed using direct volume rendering. The renderings were computed using a modified version of Simian [16] that can render arbitrary geometries into the volume rendering with correct blending. This is necessary for the in-context visualization that allows us to show the basic features of a vector field (as extracted by the moving cutting planes) together with a selection of scalar quantities. Here, it turns out that providing this kind of simultaneous visualization of different properties eases the comprehension of images that depict complicated flow structures. Moreover, interrelations between variables are derived more readily. The use of direct volume rendering and real-time transfer function modification leads to improved interactivity in the general visualization of three-dimensional flows.

The use of two-dimensional transfer functions to isolate flow features is illustrated in Figure 7. Using a transfer function of λ_2 alone (left, top image), it is possible to emphasize (in blue) the stable vortex prior to breakdown as it comes in from the left, but attempts to show the vortex bubble (in orange) are not revealing. However, adding normalized helicity as a second transfer function domain variable (the vertical axis in the transfer function widget), allows much better emphasis of the vortex bubble. Finally, by comparison with the streamline geometry, we confirm that the vortex bubble has been successfully isolated. Applying a 2D transfer function of λ_2 and helicity yields the picture of the vortical system shown on the right of Figure 7. This very intuitive visualization depicts all the key features of the flow, including primary, secondary and tertiary vortices and core regions [20, 6], as well as the surface of primary separation emanating from the sharp edge of the wing and the recirculation bubble.

Additional examples of effective visualization achieved by the developed methods are proposed in Figure 6. The upper left image shows how a combination of vortex magnitude and rotation direction in the transfer function can distinguish the vortical system above the delta wing. Although the resampling of the very fine simulation grid (11.1 million unstructured elements with very fine resolution directly above the wing) to a much coarser grid (128^3 uniform points) suggests a loss in accuracy, the vortices are cleanly separated. Asymmetric breakdown of the primary vortices is clearly visible. In the left and middle images, a close-up of the right breakdown bubble is presented. The geometry is obtained by parametric topology on a set of planes that revolve around a straight line connecting the two stagnation points related to the breakdown. The left vortex breakdown (lower row) is highly chaotic and consists of multiple recirculation zones accompanied by the typical rings.

7 Conclusion and Future Work

In this paper we have applied and extended a number of methods to advance the visualization of complicated three-dimensional flow patterns. Parametric topology tracking greatly helps in unraveling the geometry of these structures by reducing the complexity of the generated images. By modifying its original setup to permit its application to an arbitrary 1D parameter space we are able to use it for the exploration of essential flow regions along curves of interest. A subsequent application of volume rendering serves to examine variables that are derived from the flow in an intuitive and interactive manner. Through the use of multidimensional transfer functions interrelations of these variables are easily expressed and visualized. In combination with the vector field analysis provided by parametric topology it is a powerful tool that can dramatically enhance visualizations based on the composition of streamlines and isosurfaces that are typically used in practice. We have demonstrated its usefulness in examples that concerned both the verification of numerical simulations and the inquiry of the vortex breakdown phenomenon.

Future work will address following topics.

- Parametric topology need not be restricted to planes; other curved shapes could be more useful for certain problems.

- In the present work we have focused on individual time steps to investigate the features of the flow. This work must be extended to account for the time-dependency of the original data and the evolution of the visualized structures.

- Because the input data for volume rendering must typically be given in quantized form, it is essentially dimensionless and carries little connection to the original scale. This complicates the interpretation of transfer functions. Some work could be done to provide engineers with a tool more specifically tailored to their needs.

- Concerning multi-dimensional transfer function, there is still a lack of experience as to how they should be chosen appropriately or even automatically. Future research must address this limitation and further investigate the potential of direct volume rendering as a flow visualization tool in practical applications.

ACKNOWLEDGMENTS

We would like to thank Joe Kniss for providing his interactive volume rendering tool Simian [15], available at `http://www.cs.utah.edu/~jmk/simian/index.htm`. We are also thankful to Milan Ikits for his help with OpenGL. Further we thank Max Langbein, David Gruys, Alexander Wiebel and the other members of the *FAnToM* project at the University of Kaiserslautern and the University of Leipzig. Finally we thank the anonymous reviewers whose insightful comments greatly helped improve the paper.

REFERENCES

[1] M. Alexa, J. Behr, D. Cohen-Or, S. Fleischman, D. Levin, and C. Silva. Point Set Surfaces. In *Proceedings of IEEE Visualization '01*, pages 21–28, 2001.

[2] D. Banks and B. Singer. A Predictor-Corrector Technique for Visualizing Unsteady Flow. *IEEE Transactions on Visualization and Computer Graphics*, 1(2):151–163, 1995.

[3] U. Dallmann. On the Formation of Three-Dimensional Vortex Flow Structures. Technical Report 221-85 A 13, Deutsche Forschungs- und Versuchsanstalt fuer Luft- und Raumfahrt, 1985.

[4] D. Ebert, R. Yagel, J. Scott, and Y. Kurzion. Volume Rendering Methods for Computational Fluid Dynamics. In *Proceedings of IEEE Visualization '94*, pages 232–239, 1994.

[5] M. P. Escudier. Observations of the Flow Produced in a Cylindrical Container by a Rotating Endwall. *Experiments in Fluids*, 2:189 – 196, 1984.

[6] C. Garth, X. Tricoche, T. Salzbrunn, and G. Scheuermann. Surface Techniques for Vortex Visualization. In *Proceedings Eurographics - IEEE TCVG Symposium on Visualization*, May 2004.

[7] A. Globus, C. Levit, and T. Lasinski. A Tool for Visualizing the Topology of Three-DimensionalVector Fields. In *IEEE Visualization Proceedings*, pages 33 – 40, October 1991.

[8] J. L. Helman and L. Hesselink. Visualizing Vector Field Topology in Fluid Flows. *IEEE Computer Graphics and Applications*, 11(3):36–46, May 1991.

[9] J. Jeong and F. Hussain. On the Identification of a Vortex. *Journal of Fluid Mechanics*, 285:69 – 94, 1995.

[10] M. Jiang, R. Machiraju, and D. Thompson. A Novel Approach to Vortex Core Detection. In *Data Visualization 2002 (VisSym '02 Proceedings)*, pages 217 – 226. Eurographics Association, 2002.

[11] I. Jolliffe. *Principal Component Analysis*. Springer Verlag, 1986.

[12] D. N. Kenwright and R. Haimes. Vortex Identification - Applications in Aerodynamics: A Case Study. In R. Yagel and H. Hagen, editors, *IEEE Visualization '97*, pages 413–416, Los Alamitos, CA, 1997.

[13] G. Kindlmann and J. Durkin.

[14] G. Kindlmann, R. Whitaker, T. Tasdizen, and T. Möller. Curvature-Based Transfer Functions for Direct Volume Rendering: Methods and Applications. In *Proceedings IEEE Visualization 2003*, pages 513–520, October 2003.

[15] J. Kniss, G. Kindlmann, and C. Hansen. Interactive Volume Rendering Using Multi-Dimensional Transfer Functions and Direct Manipulation Widgets. In *Proceedings IEEE Visualization 2001*, pages 255–262, October 2001.

[16] J. Kniss, G. Kindlmann, and C. Hansen. Multidimensional Transfer Functions for Interactive Volume Rendering. *IEEE Transactions on Visualization and Computer Graphics*, 8(3):270–285, July-September 2002.

[17] M. Langbein, G. Scheuermann, and X. Tricoche. An Efficient Point Location Method for Visualization in Large Unstructured Grids. In *Proceedings of Vision, Modeling, Visualization*, 2003.

[18] J. Leven, J. Corso, J. Cohen, and S. Kumar. Interactive Visualization of Unstructured Grids Using Hierarchical 3d Textures. In *IEEE Symposium on Volume Visualization and Graphics*, pages 37 – 44, 2002.

[19] M. Levoy. Display of Surfaces from Volume Data. *IEEE Computer Graphics & Applications*, 8(5):29–37, 1988.

[20] H. J. Lugt. *Introduction to Vortex Theory*. Vortex Flow Press, Inc., 1996.

[21] K. Mahrous, J. Bennet, G. Scheuermann, B. Hamann, and K. I. Joy. Topological Segmentation in Three-Dimensional Vector Fields. *IEEE Transactions on Visualization and Computer Graphics*, 10(2):198–205, 2004.

[22] T. Mullin, J. J. Kobine, S. J. Tavener, and K. A. Cliffe. On the Creation of Stagnation Points Near Straight and Sloped Walls. *Physics of Fluids*, 12(2), 2000.

[23] R. Peikert and M. Roth. The "Parallel Vectors" Operator - a Vector Field Visualization Primitive. In *IEEE Visualization Proceedings '00*, pages 263 – 270, 2000.

[24] S. K. Robinson. Coherent Motions in the Turbulent Boundary Layer. *Ann. Rev. Fluid Mechanics*, 23:601 – 639, 1991.

[25] M. Roth and R. Peikert. A Higher-Order Method for Finding Vortex Core Lines. In *IEEE Visualization Proceedings '98*, pages 143 – 150, 1998.

[26] T. Satiropoulos and Y. Ventikos. The Three-Dimensional Structure of Confined Swirling Flows with Vortex Breakdown. *J. Fluid Mech.*, 26:155 – 175, 2001.

[27] W. J. Schroeder, R. Volpe, and W. E. Lorensen. The Stream Polygon: A Technique for 3d Vector Field Visualization. In *IEEE Visualization Proceedings*, 1991.

[28] D. Sujudi and R. Haimes. Identification of Swirling Flow in 3D Vector Fields. Technical Report AIAA Paper 95–1715, American Institute of Aeronautics and Astronautics, 1995.

[29] H. Theisel and H.-P. Seidel. Feature Flow Fields. In *Proceedings of Joint Eurographics - IEEE TCVG Symposium on Visualization (VisSym '03)*, pages 141 – 148. ACM, 2003.

[30] H. Theisel, T. Weinkauf, H.-C. Hege, and H.-P. Seidel. Saddle Connectors - An Approach to Visualizing the Topological Skeleton of Complex 3d Vector Fields. In *IEEE Visualization '03*, 2003.

[31] X. Tricoche, T. Wischgoll, G. Scheuermann, and H. Hagen. Topology Tracking for the Visualization of Time-Dependent Two-Dimensional Flows. *Computers & Graphics*, 26(2):249 – 257, 2002.

[32] J. J. vanWijk. Implicit Stream Surfaces. In *IEEE Visualization Proceedings*, pages 245 – 252, 1993.

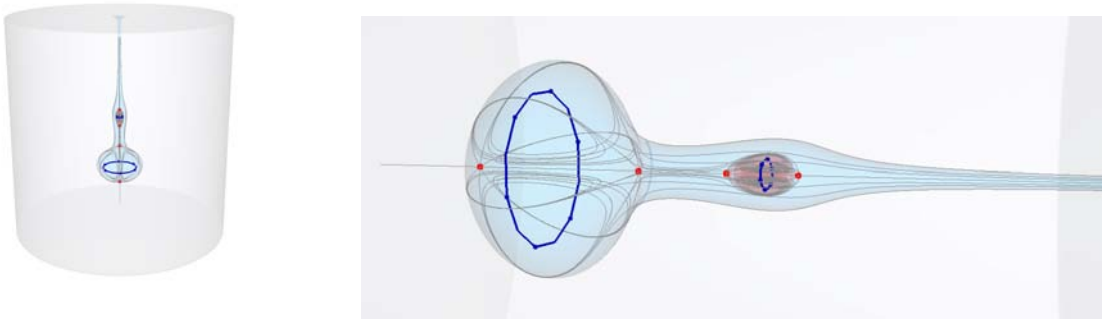

Figure 4: **Left:** An overview of the can dataset. **Right:** Parametric topology shows the essentials of vortex breakdown including the recirculation ring (blue) and a secondary vortex breakdown. To show that the separatrices accurately model the flow behavior, the breakdown bubbles are surrounded with transparent stream surfaces (light blue/light red) originating at the upstream stagnation points that are reproduced as saddle points in the topology of the planes (red).

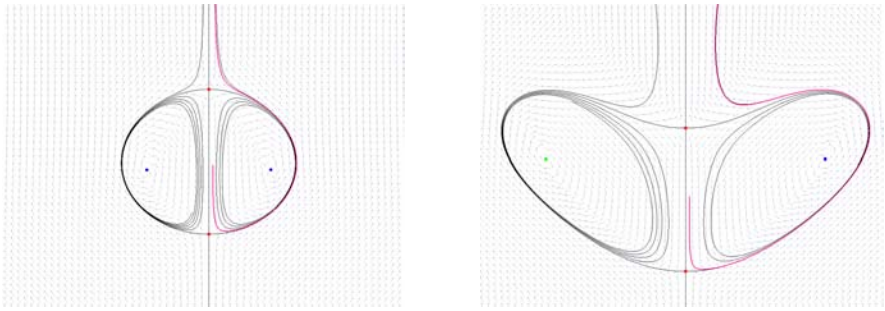

Figure 5: Can dataset feeding anomaly: the breakdown bubble is show during the growing (left) and shrinking (right) phases. The configuration of the separatrices implies that material is leaving the bubble, and a streamline (red) started inside the bubble confirms this.

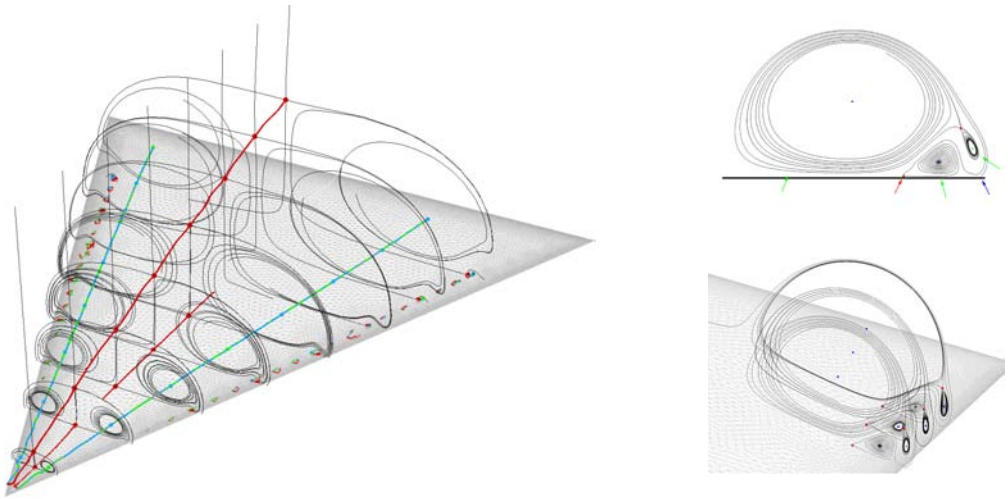

Figure 6: **Left:** An overview of the delta wing dataset: parametric topology visualizes the primary vortices. The planes are computed along the symmetry axis of the wing and are parallel. Each planes shows two sinks/sources (primary vortices) and a number of saddle points (separation from the wing). Note how the separatrices end in cycles. This indicates very weak attracting/repelling behavior of the vortices. **Right:** Primary, secondary and tertiary vortices visualized by planar topology. Here, the planes are on the primary vortex core and oriented to the flow. Note how plane orientation affects the resulting structures. Green arrows indicate the three vortices in the top image. The red arrow shows the separation sheet between primary and secondary vortex. The primary separation at the wing edge is indicated by the blue arrow. All three vortices are present as expected.

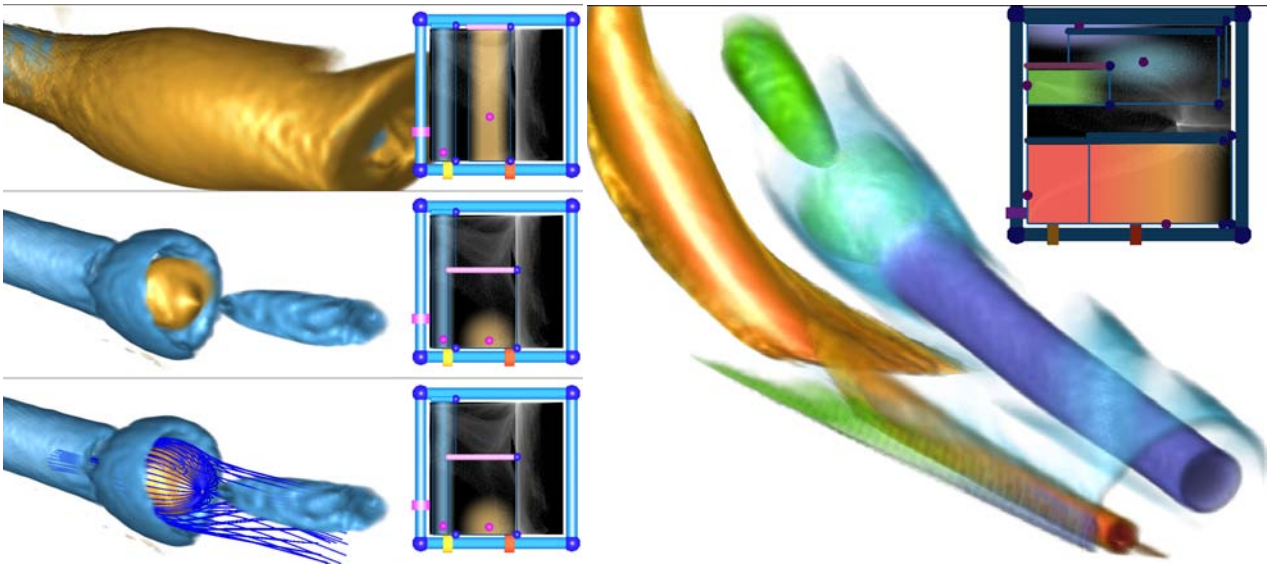

Figure 7: Use of two-dimensional transfer functions for exploration of vortical structures. **Left:** from top to bottom: 1D transfer function of λ_2 alone, 2D transfer function of λ_2 and normalized helicity, and 2D transfer function with streamline and critical point geometry. **Right:** 2D transfer function of λ_2 and helicity permits to highlight primary, secondary, and tertiary vortices along with the surface of primary separation (from the edge of the wing) and the vortex breakdown structure.

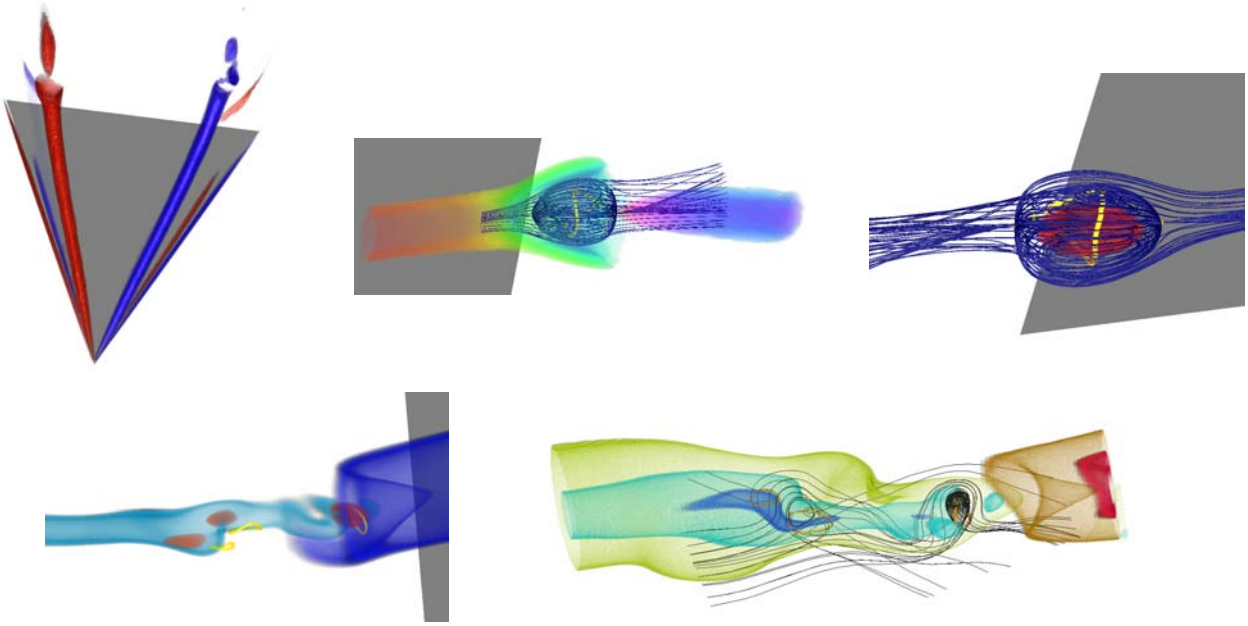

Figure 8: Volume rendering and in-context visualization on the delta wing. Through an appropriate choice of transfer function different aspects of the dataset can be visualized. The supporting geometry (planar topology) allows an exact spatial location of the volume rendered image. **Upper row:** Vortical systems of the wing, colored by direction of rotation. Note the asymmetric vortex breakdown (left). Right side vortex breakdown with a clearly visible bubble. Zones of high velocity are colored according to rotational behavior ($\lambda - 2$). High-velocity flow with slow rotation exits the breakdown bubble at the downstream end (middle). The bubble covers the recirculation (red) in the recirculation ring (yellow). The separatrices indicate that the vortex breakdown takes in material from behind (right). **Lower row:** Chaotic vortex breakdown on the left side of the wing. Zones of upstream flow (red) located near the recirculation rings obtained through parametric topology. The blue parts of the image indicate zones of high (dark) and low (light). It can be observed that the flow decelerates in a jump-like manner in front of the first recirculation zone (left). Zones of different velocities from high (red) to low (blue). Again, the jump is visible. Note the strong recirculation behavior indicated by the separatrices near the first recirculation ring (right).